1 Recent Developments in Remote Estimation of Crop Biophysical and Biochemical Properties at Various Scales

Anatoly A. Gitelson

CONTENTS

1.1 INTRODUCTION

Remote sensing has provided valuable insights into agronomic management over the past few decades. Use of remote sensing for determining crop physiological and phenological status has its roots in the pioneering work by William Allen, Harold Gausman, and Joseph Woolley [1–3], who provided much of the basic theory relating morphological characteristics of crop plants to their optical properties. These pioneering works have led to the understanding of how leaf reflectance changes in response to leaf thickness, species, canopy architecture, leaf age, nutrient and water status. Leaf chlorophyll content and its absorption in the visible spectrum provide the basis for utilizing reflectance as a tool either with broad-band radiometers or hyperspectral sensors that measure reflectance at narrow bands. The basic understanding of leaf reflectance has led to the development of various vegetation indices that have been extended to crop canopies and have been used to quantify various agronomic parameters (e.g., leaf area, crop cover, biomass, crop type, nutrient status, and yield). These tools are still being developed as we learn more about how to use the information contained in reflectance measurements from a range of different sensors.

A summary of the progress in applying remote sensing to agriculture has been published in a collection of articles in *Photogrammetric Engineering and Remote Sensing* [4–8]. Other recent reviews of the application of remote sensing methods to crops were developed by Hatfield et al. [9,10]. These articles provide a summary of the multispectral and hyperspectral remote sensing efforts in more detail and the reader is referred to these articles for a more thorough understanding.

Since first edition of this book was published [11], researchers at Center for Advanced Land Management and Information Technologies (CALMIT) at the University of Nebraska-Lincoln (UNL) have further developed and evaluated remote sensing techniques and tested them at close

range and satellite levels. This chapter contains a summary of the experiences and advances made at UNL since 2010.

1.2 VEGETATION FRACTION

One of the principal variables in the growth of crops is the fraction of the solar radiation intercepted by foliage. The productivity of crops may be analyzed as the product of the solar energy intercepted over a season and the efficiency with which that energy is converted to biomass. In many crops, the relationship between radiation interception and green foliage cover/fractional vegetation cover is sufficiently close for the latter to be used as a substitute for more elaborate measurements of light interception [11]. Thus, vegetation fraction (VF) is an important trait that helps determine crop productivity.

Different vegetation indices (VIs) for the remote estimation of VF at close range in two crop types, maize and soybean, with contrasting canopy architectures and leaf structures were evaluated [12]. To determine the accuracy of VF estimation, the noise equivalent (NE) of VF was used:

$$\text{NE}\,\Delta\text{VF} = \text{RMSE (VI vs. VF)}/[d(\text{VI})/d(\text{VF})]$$

where RMSE (VI vs. VF) and d(VI)/d(VF) are the root mean square error and the first derivative of the VI vs. VF relationship, respectively. The NE ΔVF provides a measure of how well the VI responds to VF across its entire range of its variation. NE ΔVF not only takes into account the RMSE of the VF estimation but also accounts for the sensitivity of the VI to VF, thus, providing a metric accounting for both scattering of the points from the best fit function and the slope of the best fit function.

Among the indices tested [12], the enhanced vegetation indices EVI, EVI2, wide dynamic range vegetation index (WDRVI), normalized difference vegetation index $\text{NDVI}_{\text{green}}$, and $\text{NDVI}_{\text{red edge}}$ were found to be the most accurate in estimating vegetation fraction (Figure 1.1). The algorithm for estimating VF by $\text{WDRVI} = (\alpha\rho_{\text{NIR}} - \rho_{\text{red}})/(\alpha\rho_{\text{NIR}} + \rho_{\text{red}})$ with $\alpha = 0.3$ was

$$\text{VF} = 80.84 * \text{WDRVI}_{\alpha=0.3} + 34$$

It was generic, not requiring parameterization for two crops studied with RMSE below 6% and mean normalized bias (MNB) below 2% (Figure 1.2). It was followed by red edge NDVI for both crops. EVI2 was accurate for soybeans (NE = 7.8%) and less accurate for maize (NE = 8.9%). Both $\text{VARI}_{\text{green}}$ and $\text{VARI}_{\text{red edge}}$, which were superior in estimating VF in wheat [11], were also quite accurate estimating VF in maize and soybeans; however, they were not the best among VF tested.

1.3 FRACTION OF ABSORBED PHOTOSYNTHETICALLY ACTIVE RADIATION

The fraction of absorbed photosynthetically active radiation (fAPAR) is one of the main traits used in production efficiency models (PEMs). It also plays tremendous role in accurate retrieval of light use efficiency, which is essential for assessing vegetation health. NDVI is the most-used VI for estimating fAPAR. In [13] relationships were established between fraction of PAR absorbed by photosynthetically active vegetation ($\text{fAPAR}_{\text{green}}$), and NDVI for two crops with contrasting leaf structures, photosynthetic pathways (C3 vs. C4), and canopy architectures, using *in situ* radiometric data and daily MODIS data over irrigated and rain-fed maize and soybean sites during eight years. Through the use of high temporal resolution *in situ* and MOSIS data, it was possible to identify specific phases in the growing season that aid in the interpretation of observations collected with coarser temporal resolution (or even single scenes). MODIS data are adequate for resolving distinct phases in the $\text{fAPAR}_{\text{green}}$/NDVI relationships within the growing season. The identification of these different phases has important implications for the interpretation of remotely sensed observations of crops, such as the estimation of light use efficiency (LUE) and productivity.

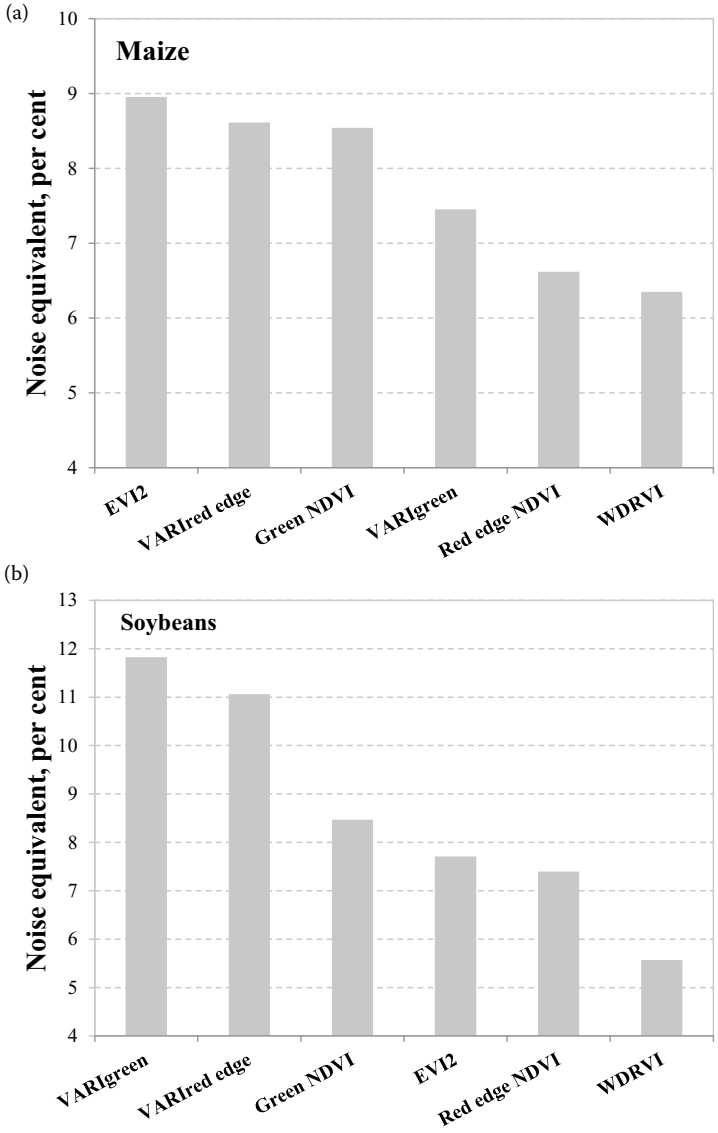

FIGURE 1.1 Noise equivalent of vegetation fraction estimation by vegetation indices tested for (a) maize, five years, nine irrigated and rain-fed sites; and (b) soybeans, three years, six irrigated and rain-fed sites.

Significantly, in [13] was shown that established relationships of $fAPAR_{green}$ vs. *in situ* NDVI were very close to that of $fAPAR_{green}$ vs. MODIS-retrieved NDVI. In vegetative stages, when $fAPAR_{green}$ was below 0.65, the $fAPAR_{green}$/NDVI relationships for crops with contrasting leaf structures and canopy architecture were close and almost linear, allowing accurate estimation of $fAPAR_{green}$ with RMSE = 5.8% (Figure 1.3). However, $fAPAR_{green}$/NDVI relationships in reproductive stages were very different for both crops (Figure 1.4), showing that canopy architecture and leaf structure greatly affect the relationship as leaf chlorophyll (Chl) content changes and vertical distribution of Chl content and green leaf area index (LAI) inside the canopy becomes heterogeneous.

The study [13] revealed fine details of the $fAPAR_{green}$/NDVI relationships, specifically two types of hysteresis that prevent accurate $fAPAR_{green}$ estimation using NDVI during the whole growing season. SAIL (Scattering by Arbitrary Inclined Leaves) model simulations of the $fAPAR_{green}$/NDVI

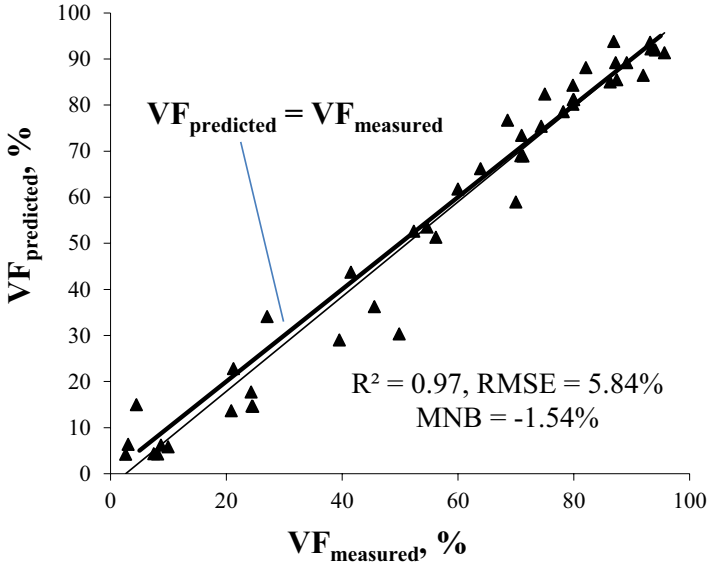

FIGURE 1.2 Vegetation fraction VF predicted by WDRVI with $\alpha = 0.3$ plotted versus vegetation fraction measured in irrigated and rain-fed maize and soybeans sites.

relationship for maize clearly displayed the existence of hysteresis in the relationship as revealed by empirical data.

It was also found that the $fAPAR_{green}$/NDVI relationships, established for vegetative stages in maize and soybean, are very different from other empirical studies at close range and satellite levels as well as from radiative transfer simulations [13]. This shows need for extensive research in

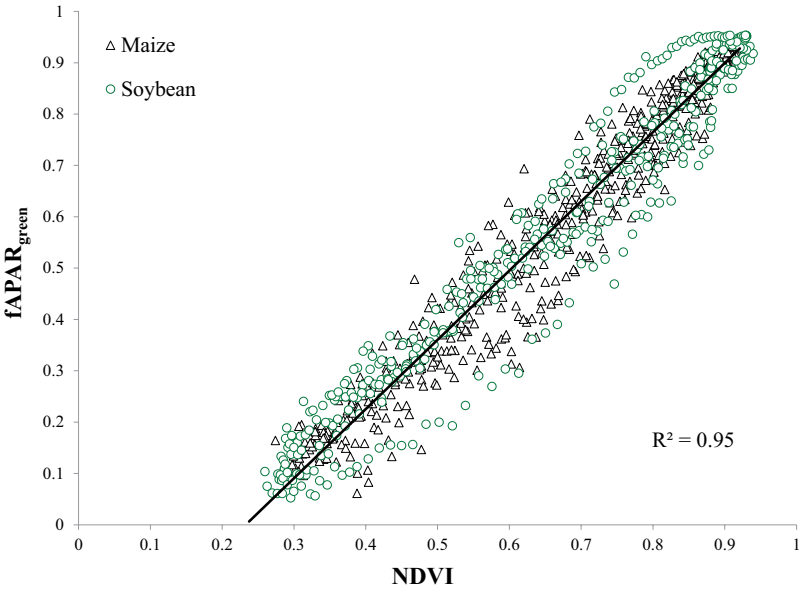

FIGURE 1.3 The MODIS-retrieved $fAPAR_{green}$/NDVI relationships for maize (collected in 2001 through 2008 in irrigated and rain-fed sites) and soybean (collected in 2002, 2004, 2006, and 2008 over two irrigated and rain-fed sites each year) in vegetative stage only (700 observations). Solid line is best-fit function.

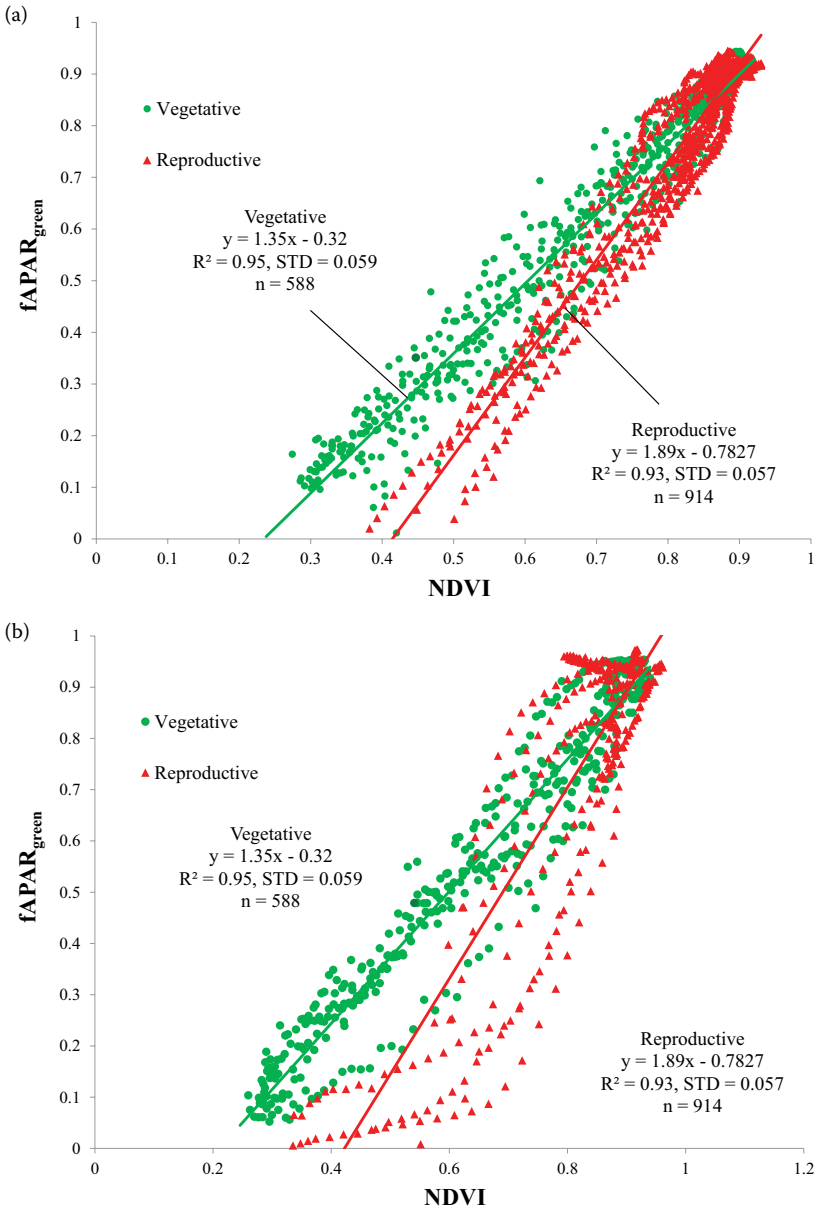

FIGURE 1.4 MODIS-retrieved NDVI vs. $fAPAR_{green}$ relationships for (a) maize in 2001 through 2008 (16 site years) and (b) soybean in 2002, 2004, 2006, and 2008 (8 site years).

remote sensing techniques for $fAPAR_{green}$ estimation. The issues of canopy vertical heterogeneity (in terms of leaf Chl content, leaf area, and leaf angle distribution), studied in [13], also affect other remote sensing problems such as estimating leaf and canopy Chl content, light use efficiency, and productivity. However, there has been little work addressing the issue of the effects of vertical variability in canopy structure and the paper [13] shows the importance of this.

In order to develop generic algorithms for $fAPAR_{green}$ estimation, VIs previously used for fAPAR estimation were tested. The reflectance spectra collected at close range [11] were resampled to spectral bands of the Moderate Resolution Imaging Spectroradiometer (MODIS) (green 545–565 nm, red 620–670 nm, and NIR 841–876 nm) using MODIS spectral response function and SR (simple ratio),

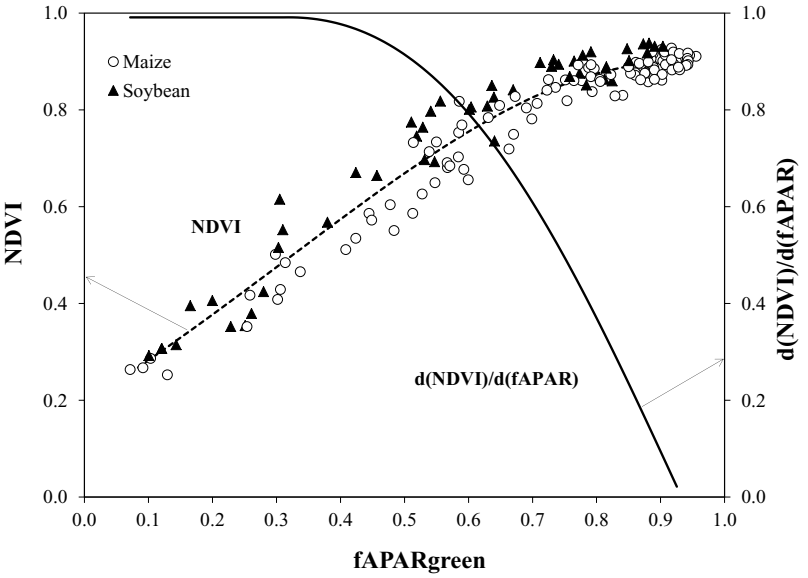

FIGURE 1.5 NDVI calculated with reflectance in spectral bands of MODIS and first derivative of NDVI with respect to $fAPAR_{green}$ plotted vs. $fAPAR_{green}$ in maize and soybean. Dashed line is best-fit function for NDVI vs. $fAPAR_{green}$ relationship.

NDVI, EVI2, TVI, MTVI1, MTVI2, $VARI_{green}$, OSAVI, WDRVI with $\alpha = 0.5$, and Green NDVI were calculated. The reflectance spectra were also resampled to spectral bands of the Multi Spectral Instrument (MSI) on the Sentinel-2 satellite system (green: 550–580 nm, red: 660–670 nm, red edge 1: 693–712 nm, red edge 2: 732–748 nm and NIR: 773–793 nm) using MSI spectral response function and MTCI, $VARI_{erd\ edge}$, red edge NDVI were calculated.

The relationship between NDVI and $fAPAR_{green}$ was almost non-species-specific (Figure 1.5). Thus, NDVI is supposed to be a proxy of $fAPAR_{green}$. However, the NDVI/$fAPAR_{green}$ relationship is asymptotic, with a decrease in the slope as $fAPAR_{green}$ exceeds 0.7 (first derivative dNDVI/df$APAR_{green}$ in Figure 1.5). Thus, NDVI exhibits limitations at moderate-to-high vegetation density. As $fAPAR_{green} > 0.7$, RMSE of $fAPAR_{green}$ estimation by NDVI grows exponentially, reaching 0.25 for $fAPAR_{green} = 0.8$. This means that in crop studied for more than two months during the growing season NDVI does not yield reliable information about $fAPAR_{green}$ [11].

EVI and EVI2 were closely related to $fAPAR_{green} < 0.7$, but further increase of EVI from 0.6 to 0.9 did not relate to $fAPAR_{green}$ (Figure 1.6). For the crops studied, the slope of $fAPAR_{green}$/LAI and $fAPAR_{green}$/[Chl] relationships increased gradually until LAI reached 3–4 and then it dropped due to decrease in depth of light penetration inside the canopy and decrease of Chl efficiency in light absorption [14]. Thus, for LAI > 3, EVI2 did follow the increase in LAI while $fAPAR_{green}$ increased a little, which disturbs the close $fAPAR_{green}$/EVI relationship.

Among VIs tested, only three had close linear non-species-specific relationships with $fAPAR_{green}$: WDRVI with $\alpha = 0.5$, green NDVI, and red edge NDVI. All three VIs were developed to avoid NDVI's limitation of estimating biophysical characteristics of dense vegetation. The main reasons for decreasing NDVI sensitivity to high-density vegetation are (i) a high ρ_{NIR}/ρ_{red} ratio that reaches 7–10 for moderate-to-high density vegetation, and (ii) saturation of red reflectance. WDRVI is a modification of NDVI that attenuates the effect of near infrared (NIR) reflectance by $\alpha < 1$. It makes the magnitudes of $\alpha\rho_{NIR}$ and ρ_{red} comparable and increases the sensitivity of WDRVI to such traits of dense vegetation as vegetation fraction and LAI. The $fAPAR_{green}$/$WDRVI_{\alpha=0.5}$ relationship was not species specific, with $R^2 = 0.92$ ($p < 0.001$) and RMSE = 0.069 (Figure 1.7, Table 1.1). Interestingly that close relationship between WDRVI and $fAPAR_{green}$ for Soil-Canopy Observation

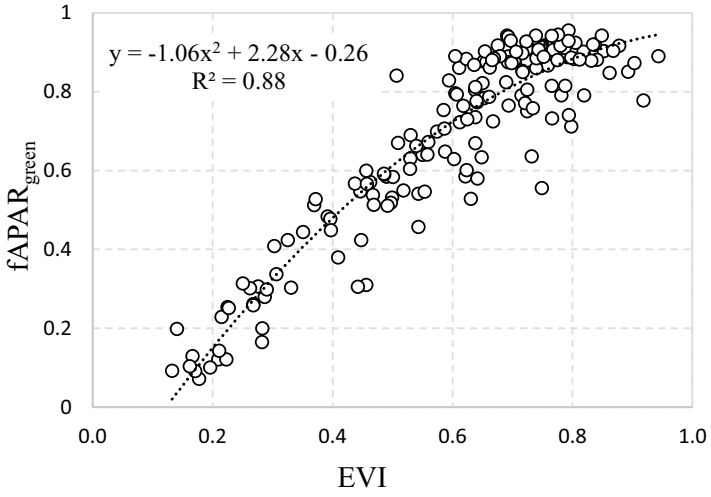

FIGURE 1.6 Relationship between $fAPAR_{green}$ and EVI2 for maize and soybean.

of Photosynthesis and Energy (SCOPE) simulations with LAI varying from 1 to 4, leaf chlorophyll content (20–80 μg/cm^2), solar zenith angle 20–60°, and three typical leaf inclination distribution functions (planophile, plagiophile, and spherical) was recently found [15].

The use of green and red edge spectral bands instead of red in NDVI is another way to increase the sensitivity of NDVI-like vegetation indices to traits of high-density vegetation. The absorption

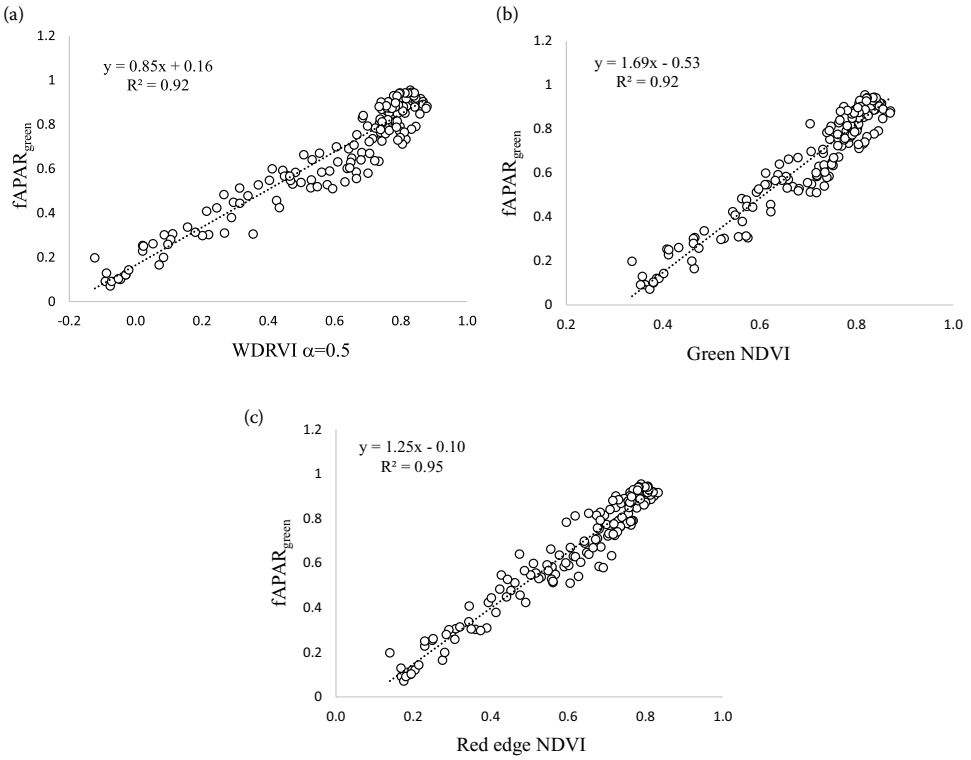

FIGURE 1.7 $WDRVI_{\alpha=0.5}$ (a), green NDVI (b), and red edge NDVI (c) plotted versus $fAPAR_{green}$ for maize and soybean.

TABLE 1.1
Algorithms, Determination Coefficients (R^2), and RMSE of $fAPAR_{green}$ Estimation in Maize and Soybean by Vegetation Indices

VI	$fAPAR_{green}$ vs. VI	R^2	RMSE
EVI	$y = -1.06x^2 + 2.28x - 0.26$	0.88	0.096
NDVI	$y = 0.07\exp(2.81x)$	0.92	0.075
WDRVI, $\alpha = 0.5$	$y = 0.85x + 0.16$	0.92	0.069
Green NDVI	$y = 1.6891x - 0.5271$	0.92	0.067
Red edge NDVI	$y = 1.2531x - 0.1035$	0.95	0.057

Note: The vegetation index names are given in full in the text. fAPAR, fraction of absorbed photosynthetically active radiation. RMSE, root mean square error.

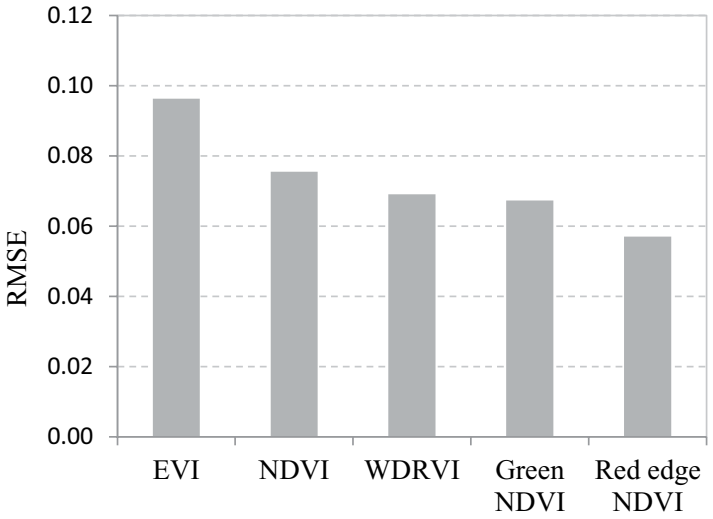

FIGURE 1.8 Root mean square error of $fAPAR_{green}$ estimation using different vegetation indices.

coefficient of Chl in the green and red edge spectral regions, located far from the main red absorption band of Chl (*in situ* around 670 nm), is not higher than 1%–2% of that in the red and the pathway of light inside a leaf and canopy is much larger than in the red. So, with increase in vegetation density, absorbance in these spectral regions continues to increase, enhancing sensitivity of the green and red edge reflectance to $fAPAR_{green}$.

The relationships of $fAPAR_{green}$ vs. green NDVI and $fAPAR_{green}$ vs. red edge NDVI were found to be very close ($p < 0.001$) with $R^2 = 0.92$ and 0.95, respectively (Figure 1.7). Red edge NDVI appears to be the best index for $fAPAR_{green}$ estimation in the whole range of its variation (Figure 1.8). The algorithms presented in Table 1.1 are not species specific for maize and soybean and do not require parameterization for these crops.

1.4 CHLOROPHYLL AND NITROGEN CONTENT

Canopy chlorophyll content (Chl) relates closely to plant photosynthetic capacity, nitrogen status, and productivity, and the necessity of remote Chl estimation in crops is recognized (e.g., [14,16]). Seasonal changes in the pigment pool and structural canopy properties greatly influence the light climate

inside the canopy and modulate the extinction coefficient. For realistic modeling of reflectance, radiative transfer models should be fed by known vertical LAI and pigment content distributions as well as their changes during the season. It is important for monitoring crops with different structural properties when the spatial resolution of the sensor is low (e.g., comparable to field size or larger) and in regions with mixed-use cropping practices (e.g., maize/soybean rotation) requiring generic algorithms that do not need reparameterization for different crops.

Development of generic algorithms for Chl estimation that could be applied with no reparameterization for two contrasting crop species, maize and soybean, during the entire growing season was a goal of Peng et al. [16]. These two crops represent different biochemical mechanisms of photosynthesis, leaf structure, and canopy architecture. The relationships between canopy Chl and reflectance, collected at close range and resampled to bands of the Multi Spectral Instrument (MSI) aboard Sentinel-2, were analyzed in samples taken across the entire growing seasons in irrigated and rain-fed sites located in eastern Nebraska between 2001 and 2005.

Crop phenology was found to be a strong factor influencing canopy reflectance in two contrasting crops. Phenology caused a substantial species-specific difference (hysteresis) in the reflectance vs. canopy Chl relationships between the vegetative and reproductive stages. The reasons for the hysteresis were seasonal changes in canopy architecture, leaf structure, and foliar Chl, as well as seasonal changes in the influence of the soil/residue background. The effect of the hysteresis on vegetation indices applied for canopy Chl estimation depended on the bands selected in their formulation. For widely used VIs using NIR and red reflectance, NDVI, SR and EVI, there were significant differences in the VI vs. canopy Chl relationships between the vegetative and reproductive stages and between species, limiting their application for accurate canopy Chl estimation over the entire growing season. VIs with red edge and NIR bands, using reflectance simulated for the MSI sensor, included the chlorphyll index $CI_{740} = (\rho_{NIR}/\rho_{740}) - 1$, MERIS terrestrial chlorophyll index $MTCI = (\rho_{NIR} - \rho_{705})/(\rho_{705} - \rho_{670})$, and red edge $NDVI_{740} = (\rho_{NIR} - \rho_{740})/(\rho_{NIR} - \rho_{740})$. These VIs were accurate in estimating canopy Chl in maize and soybean with RMSE values below 0.38 g m^{-2} (Figure 1.9, Table 1.2). Algorithms utilizing these VIs require neither parameterization for each crop nor for each phenological stage (Table 1.2).

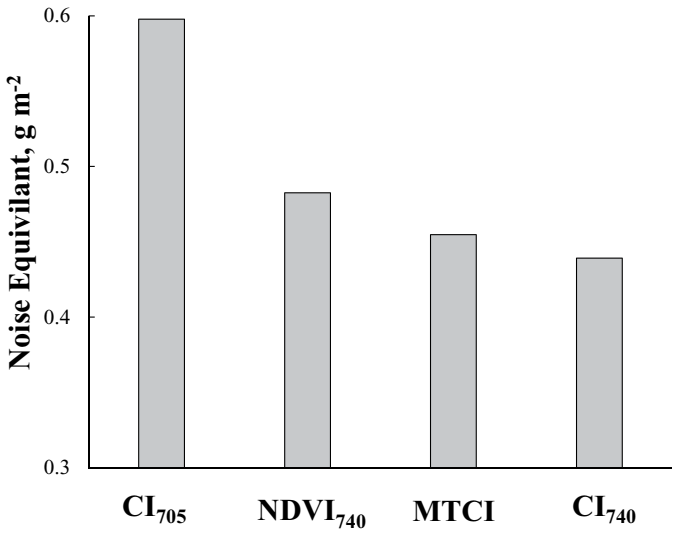

FIGURE 1.9 Noise equivalent of canopy Chl content estimation in maize and soybean combined by vegetation indices calculated using reflectance simulated at MSI spectral bands for chlorophyll index with red edge band at 705 nm (CI_{705}), red edge NDVI with red edge band at 740 nm ($NDVI_{740}$), MTCI, and chlorophyll index with red edge band at 740 nm (CI_{740}). Data taken from 2001 through 2005 over three irrigated and rain-fed sites (11 maize sites years and 4 soybeans sites year) with Chl content varied from 0 to 4.5 g m^{-2}.

TABLE 1.2
Algorithms for Canopy Chlorophyll Content Estimation, Generic for Maize and Soybean, Determination Coefficients (R^2), and RMSE in g m^{-2} for Three Vegetation Indices

Canopy Chl in g m^{-2}	R^2	RMSE
Chl = 0.241 × MTCI – 0.618	0.90	0.38
Chl = 18.509 × (red edge $NDVI_{740}$) – 0.999	0.91	0.37
Chl = 6.645 × CI_{740} – 0.649	0.91	0.36

Note: The vegetation index names are given in full in the text. Chl, chlorophyl content. RMSE, root mean square error.

Development of generic algorithms for canopy Chl estimation in rice, wheat, corn, soybean, sugar beet, and natural grass using red edge and NIR spectral bands was presented in Inoue et al. [17]. The ratio of reflectances at 815 and 704 nm (ρ_{815}/ρ_{704}) was found to be superior to all other models in overall predictive ability of canopy Chl content. The soundness of the model was supported by simulation analyses using a radiative transfer model under various canopy conditions including plant types (canopy geometry), leaf Chl content, LAI, and soil background. Importantly, the partial least squares regression (PLSR) and interval partial least squares regression (iPLSR) models using much larger number of wavebands proved to be inferior to the VI-based models, especially in versatility.

The authors of Ciganda et al. [18] addressed a very important question: how deep into the maize canopy is Chl content sensed by the red-edge chlorophyll index, $CI_{red\ edge}$? Statistical techniques, a hierarchical regression, and three Aikaike Information Criterion, were used to determine how many leaf layers are sensed by the $CI_{red\ edge}$. The hierarchical regression procedure made it possible to assess the importance of each leaf Chl content in defining total Chl content in a maize canopy and documented very close relationships between $CI_{red\ edge}$ and total canopy Chl content when 8 to 10 top leaf layers were included in the model. Such deep sensing inside the maize canopy is the reason for the high accuracy in estimating maize canopy Chl content by $CI_{red\ edge}$, which employed the NIR and the red-edge (720–730 nm) spectral bands.

A strong correlation between foliar nitrogen (N) and Chl contents has been found for various plant species [19–21]. Since Chl is the main plant constituent determining the reflectance in the visible region of the spectrum, optical remote sensing techniques have great potential in providing information on canopy Chl and N content. Baret et al. [19] suggested that canopy Chl content is well suited for quantifying canopy level N content. Canopy Chl content is a physically sound quantity that represents the optical path in the canopy where absorption by Chl dominates the radiometric signal. Thus, absorption by Chl provides the necessary link between remote sensing observations and canopy-state variables that are used as indicators of N status and photosynthetic capacity.

PROSAIL (PROSPECT and Scattering by Arbitrary Inclined Leaves) simulations showed that the $CI_{red\ edge}$ is linearly related to the canopy Chl content over the full range of potential Chl values [22]. In that paper, the best results in estimating either canopy Chl or N content were obtained using $CI_{red\ edge}$ and CI_{green}. It was also shown that the precise position of the spectral bands in the $CI_{red\ edge}$ is not very critical. In [23], this was further elaborated by studying the spectral bands to be used in the $CI_{red\ edge}$ in order to get the minimum RMSE in estimating canopy Chl and N content for three crop species (potato, maize, and soybean) and grass. Although results varied for the various experiments, optimal results were obtained using a spectral band around 800 nm in the numerator of the $CI_{red\ edge}$ and a spectral band in the range 705–740 nm in the denominator. The choice of the denominator waveband was more critical than the choice of the numerator: for maize and grass (erectophile canopies) this was in a wide range of 720–740 nm, whereas for soybean and potato (planophile

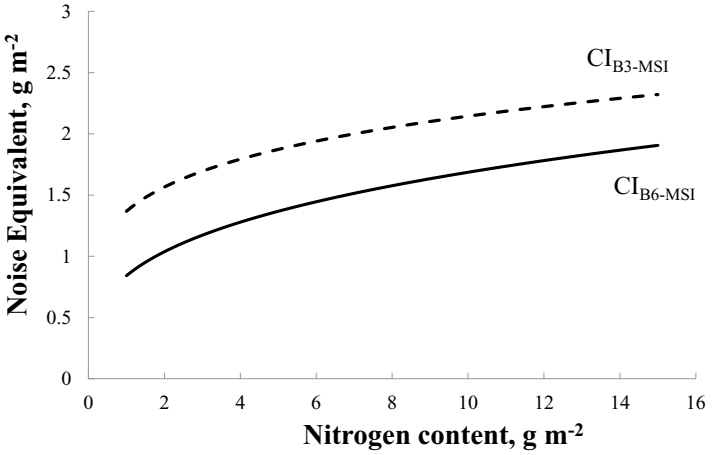

FIGURE 1.10 Noise equivalent of total nitrogen content estimation in maize by green and red edge chlorophyll indices (CI_{green} and $CI_{red\ edge}$), calculated using green B3 (543–577 nm) and red edge B6 (732–747 nm) spectral bands of MSI sensor onboard Sentinel-2. (From Schlemmer, M. et al., *International Journal of Applied Earth Observation and Geoinformation*, 25, 47–54, 2013. [24])

canopies) this band was around 705–710 nm. Subsequently, the Sentinel-2 spectral bands have been simulated using the data of the four experiments. In all experiments, the best results in estimating canopy Chl and N content were obtained using the $CI_{red\ edge}$, CI_{green}, and MTCI. Moreover, results using the Sentinel-2 band positions were quite similar to the optimal band positions for the $CI_{red\ edge}$. This confirms the importance of the red edge bands on Sentinel-2. However, CI_{green} with green band presented in MODIS and Landsat also seems very promising and requires further research.

In Schlemmer et al. [24] was shown that Chl and N content in maize can be estimated by the same remote sensing techniques, confirming a paradigm that absorption by Chl provides the necessary link between remote sensing observations and canopy-state variables that are used as indicators of N status. The study [24] presented the significance of the green (560 nm) and long-wave red edge (740 nm) bands of the MSI sensor on Sentinel-2 for estimating Chl and N contents in maize (Figure 1.10). Also notable, $CI_{red\ edge}$ with quite a wide spectral band around 740 nm was optimal for N and Chl estimation. $CI_{red\ edge}$ with red edge band 720–730 nm allowed accurate non-species-specific estimation of gross primary production in maize and soybean [11,16] and the same range was found to be optimal for N estimation in rice [25]. Thus, it is likely that presented techniques for N and Chl estimation in maize could accurately estimate the same characteristics in other crops.

Despite encouraging results, thoughtful studies of reflectance vs. canopy Chl relationships are still required for different types of crops with contrasting biochemical and structural properties. The robustness of generic algorithms for different crops and their varieties should be confirmed in further studies. These algorithms should also be examined for their sensitivity to a range of typical soil backgrounds.

1.5 GREEN LEAF AREA INDEX

One of the key traits affecting primary production is the green leaf area index (green LAI), which is the ratio of the one-sided green leaf area to the ground area underneath. NDVI is widely used for estimating green LAI (see for review [10,26]). However, the relationship between NDVI and green LAI is essentially nonlinear and exhibits significant variations among various vegetation types. When green LAI > 2, NDVI is generally insensitive to green LAI. Thus, the main requirements for remote sensing techniques estimating green LAI are (i) increase of sensitivity to moderate-to-high

vegetation density and (ii) decrease of their sensitivity to leaf structure and canopy architecture. Both issues are addressed below.

Remote sensing techniques for estimating green LAI in two crop types (maize and soybean) with contrasting canopy architectures and leaf structures were evaluated to develop algorithms not requiring reparameterization for each crop [26]. Among the VIs tested, the CI_{green}, the $CI_{red\ edge}$ and the MTCI exhibited strong and significant linear relationships with green LAI ranging from 0 to more than 6 m^2/m^2. The $CI_{red\ edge}$ was the only index insensitive to crop type and produced the most accurate estimations of green LAI in both crops (RMSE < 0.58 m^2/m^2). These results were obtained using data acquired at close range (i.e., field spectrometers mounted 6 m above the canopy) and from an aircraft-mounted Airborne Imaging Spectrometer for Applications (AISA). As the $CI_{red\ edge}$ also exhibited low sensitivity to soil background effects, it constitutes a simple yet robust tool for the remote and synoptic estimation of green LAI.

In [27] the results of the development of generic algorithms for green LAI estimation in four different crops, maize, soybean, wheat, and potato, were presented. Spectral measurements and green LAI data of wheat and potato were obtained in Israel and of maize and soybean in the United States. Among the VIs examined, two variants of the chlorophyll index (CI) and WDRVI with the green and red edge bands were the most accurate in estimating green LAI in all four crops. Hyperspectral reflectance data were used to determine optimal diagnostic bands for estimating green LAI in four crops using a universal algorithm. The green (530–570 nm) and red edge (700–730 nm) regions were identified as having the lowest errors in estimating green LAI. Since the Landsat 8 Operational Land Imager (OLI) has a green spectral band and the Sentinel-2, Sentinel-3, and VENμS have both green and red edge bands, it is expected that these VIs can be used to monitor green LAI in multiple crops using a single algorithm.

VIs that are maximally sensitive to green LAI along its entire range of variability were presented in [28]. In order to benefit from the different sensitivities of VIs along the entire green LAI range, combining of VIs was suggested. For sensors with spectral bands in the red and NIR regions, the best combination was NDVI and SR (maize normalized root mean square error (NRMSE) = 10%; soybean NRMSE = 11.5%). However, this combined index was species specific. For sensors with bands in the red edge and NIR regions, the best combination was red edge NDVI and $CI_{red\ edge}$, not requiring reparameterization, and was capable of accurately estimating green LAI in both crops (i.e., maize and soybean) with a NRMSE below 10%.

Informative spectral bands for estimating green LAI in maize (a C4 species) and soybean (a C3 species) retained in three types of methods—neural networks (NN), partial least squares (PLS) regression, and vegetation indices (VI)—were found in [29]. Hyperspectral reflectance and green LAI of irrigated and rain-fed maize and soybean were taken during eight years of observations (altogether 24 site-years) in very different weather conditions. The red edge and the NIR bands were selected by all methods and were found to be the most informative. The best results were obtained with NN using four spectral bands—two on red edge (700–710 and 720–740 nm), NIR (beyond 770 nm), and red (around 670 nm)—with NRMSE $< 7.7\%$. These were followed by $CI_{red\ edge}$, using red edge and NIR bands, and PLS using three bands, both with NRMSE $< 8.5\%$.

The validity of these bands was further confirmed via the uninformative variable elimination PLS technique, UVE PLS [30,31]. This technique assists in reducing the data dimension by eliminating spectral data that are uninformative or redundant and identifying the most informative spectral regions of the hyperspectral data. A smaller absolute value of the reliability parameter indicates that the data are less informative and can be removed at the user's discretion. Centner et al. [31] cautioned that this approach is not for band selection, but it is a way to eliminate variables that are useless. The most informative spectral bands for green LAI estimation were found by UVE PLS in the NIR, red edge, and green spectral ranges (Figure 1.11).

Informative spectral bands for green LAI estimation in maize and soybean using spectral data taken at close range [29] were tested in [32–34] using Aqua and Terra MODIS, Landsat TM

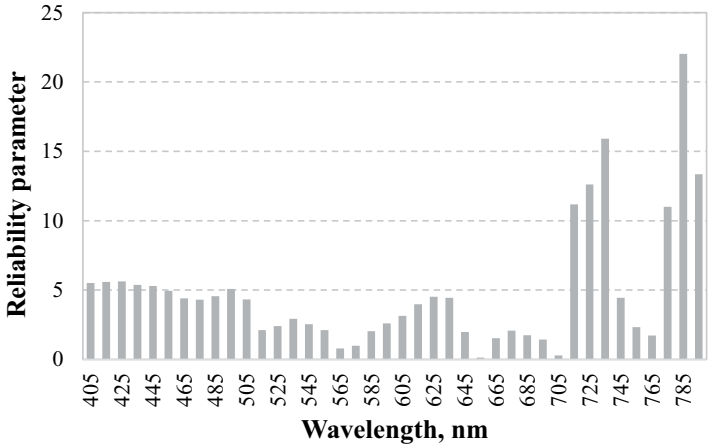

FIGURE 1.11 Spectra of reliability parameter calculated using hyperspectral data taken 6 m above the top of canopy and green LAI in maize and soybean combined by uninformative variable elimination partial least-squares (UVE PLS) technique. The magnitude of the reliability parameter is an indicator of useful information contained in reflectance spectra.

and ETM+, ENVISAT MERIS surface reflectance products, and simulated data of the recently launched Sentinel-2 MSI and Sentinel 3 OLCI (Ocean and Land Colour Instrument). Special emphasis was placed on testing generic algorithms that not require reparameterization for these species. Four techniques were investigated in [32]: support vector machines (SVM), neural network (NN), multiple linear regression (MLR), and vegetation indices (VI). All models tested provided a robust and consistent selection of spectral bands related to green LAI in crops representing a wide range of biochemical and structural traits. For TM/ETM+ Landsat, when only two spectral bands were allowed, all four techniques selected green and NIR bands. Among the nonparametric regression techniques, NN and SVM were the best with NRMSE below 14.4%. Addition of a third band (in the blue region) decreased the NRMSE only slightly (to 14%). When four bands were used (the fourth band was in the red region), NRMSE increased, due likely to overfitting at the training stage. WDRVI with two bands, green and NIR, was able to estimate green LAI with NRMSE below 13%.

The smallest NRMSEs of LAI estimation around 11.8% for all three techniques (MLR, SVM, and NN) were obtained using MERIS data. To achieve this accuracy, SVM used only three bands and addition of a fourth band decreased accuracy. In contrast, MLR reached maximal accuracy using five bands and NN six bands. However, when the fifth and sixth bands were added, the reduction in NRMSE was very small (0.1%–0.25%). WDRVI with two bands, red edge and NIR, achieved NRMSE $< 12\%$ and explained more than 83% of LAI variation in the two crops taken together (Figure 1.12). Sentinel-2 MSI and Sentinel 3 OLCI estimates based on simulated data had NRMSE below 8%. However the accuracy of these models with actual MSI and OLCI surface reflectance products remains to be determined.

These findings lay a strong foundation for the development of generic algorithms that are crucial for remote sensing of vegetation biophysical parameters. The bands retained by SVM, NN, PLS, and VI were in close agreement and were confirmed in [35] by Gaussian processes regression where top performances were found with between four and nine bands, and all of them relied on a band in the red edge and other bands in relevant absorption regions. Identifying informative spectral bands across all four techniques provided insight into spectral features of reflectance specific for each species as well as those that are common to species with different leaf structures, canopy architectures, and photosynthetic pathways.

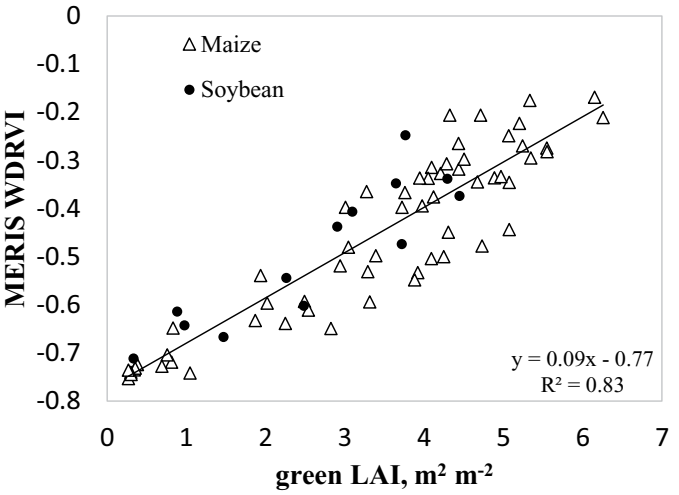

FIGURE 1.12 Relationships between MERIS WDRVI and green LAI in maize and soybean. WDRVI was calculated using MERIS (red edge and NIR) surface reflectance products. MERIS data were collected in 2003–2011 (61 images over maize and 14 over soybean). NRMSE < 12%. (From Kira, O. et al., *Remote Sensing*, 9, 318, 2017, doi: 10.3390/rs9040318. [32])

1.6 GROSS PRIMARY PRODUCTION

Vegetation productivity is the basis of all the biospheric functions on the land surface and is defined as the production of organic matter through photosynthesis. The total amount of organic matter produced through photosynthesis is termed the gross photosynthesis, and if expressed as the integral of the organic matter produced by all the individual plants in a defined area per unit of time, is termed the gross primary productivity (GPP). Given that the vegetation productivity is directly related to the interaction of solar radiation with the plant canopy [9–11], remote sensing techniques are used to measure vegetation productivity.

In the first CALMIT/UNL publications on remote estimation of crop GPP it was hypothesized that crop photosynthesis and GPP relate closely to total canopy/stand Chl content and thus that GPP can be estimated remotely using Chl-related models [11]. Using limited data sets it was shown that GPP could be estimated accurately by vegetation indices closely related to Chl content ($CI_{red\ edge}$, MTCI and CI_{green}). Rational for the hypothesis was (Figure 1.13): (i) fAPAR vs. Chl relationship was essentially not linear with significant (more than 5-fold) decrease of slope as Chl > 2 g m^{-2} and the slope was close to zero for Chl > 3 g m^{-2} (Figure 1.13a); (ii) in contrast to fAPAR, with increase in Chl above 2 g m^{-2} GPP steadily increased (Figure 1.13b), so GPP was sensitive to Chl content despite substantial decrease of fAPAR sensitivity to Chl; (iii) light use efficiency was found to be related to Chl content (Figure 1.13c) and it explained high sensitivity of GPP to moderate-to-high Chl (see [36–38] for detail).

This new paradigm based on total Chl content was elaborated using multiyear data taken over maize and soybean at three irrigated and rain-fed AmeriFlux sites in Nebraska, USA [36–38]. A model was suggested relating crop GPP to a product of total canopy Chl content and incoming photosynthetically active radiation, PAR_{in} [37–38]. Canopy Chl content was estimated by VIs closely related to Chl content. It was shown that the Chl–PAR_{in} model was able to accurately estimate GPP using VIs retrieved from reflectance data taken at close range over maize, soybean, and wheat [11,37–38] as well as grassland [39].

For application of the model for estimating GPP in C3 and C4 crops with no parameterization of algorithms, two questions were addressed: (i) Are the algorithms developed for maize and soybean

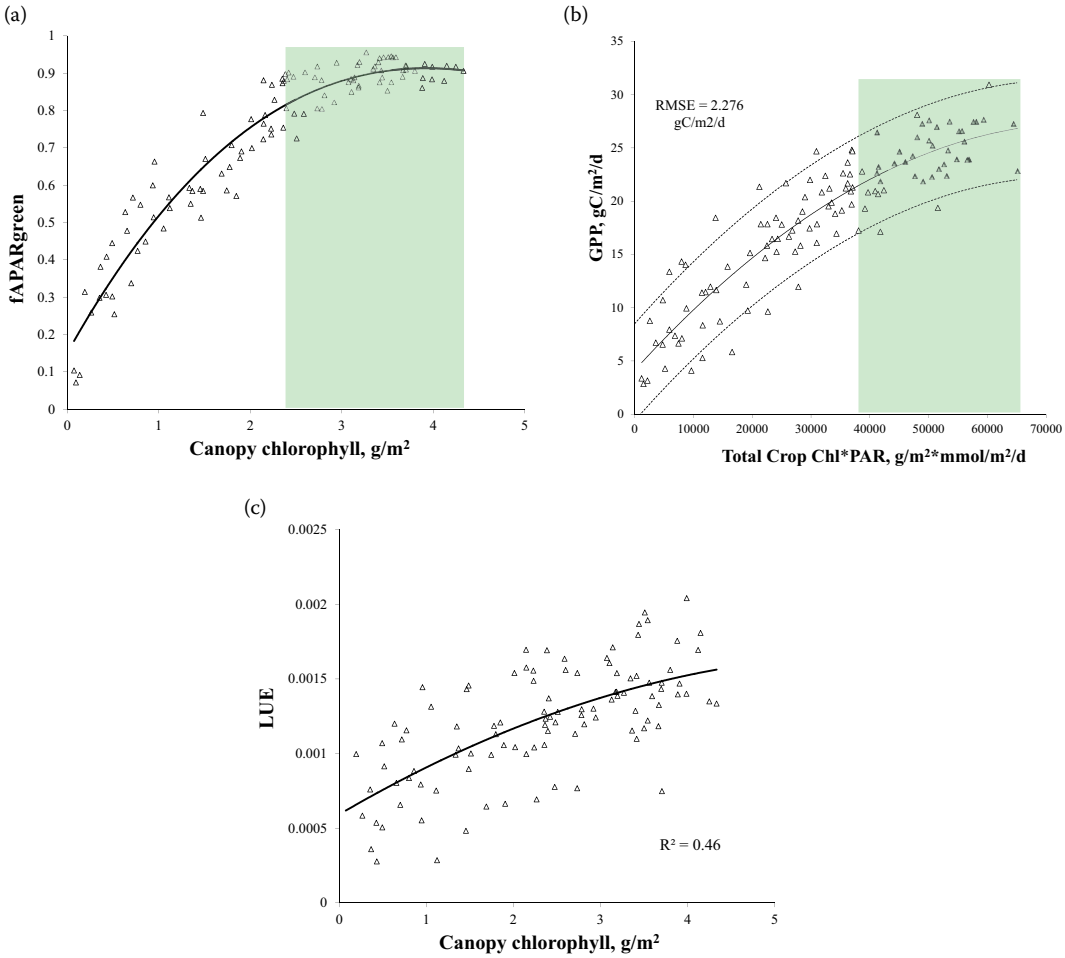

FIGURE 1.13 Fraction of PAR absorbed by photosynthetically active vegetation ($fAPAR_{green}$) (a), gross primary production (GPP) (b), and light use efficiency (LUE) (c) plotted versus canopy Chl content in maize. Hyperspectral reflectance data (110 observations) were taken at close range and GPP was measured at three AmeriFlux irrigated and rain-fed sites in Nebraska in 2001 through 2005.

different? (ii) Is it possible to develop a unified generic algorithm for GPP estimation in both maize and soybean? It was shown that several VIs may be used for generic GPP assessment—Figure 1.14 [37–38]. The use of red edge NDVI, red edge WDRVI, CI_{green} and $CI_{red\ edge}$ allowed for estimation of GPP in both crops with no parameterization, with NRMSE $< 10\%$. However, *only* $CI_{red\ edge}$ *and red edge NDVI were not species specific for maize and soybean.*

To apply the model for estimating crop GPP to satellite data, three approaches were used with respect to PAR: (i) incident PAR (PAR_{in}), (ii) PAR retrieved from short-wave radiation data [40], and (iii) potential photosynthetically active radiation (PAR_{pot}) [41–42]. PAR_{pot} is the PAR_{in} value under conditions of minimal aerosol loading; it represents the seasonal changes in hours of sunshine (i.e., day length). It was shown that the use of a product of Chl-related VI and PAR_{pot} gave significantly decreased uncertainties of GPP estimation compared with other approaches [41–43].

Concurrent GPP and TM/ETM+ Landsat observations during 2001–2008 over the three Nebraska AmeriFlux sites represented a wide range of GPP variation (maize GPP ranging from 0 to 31 gC/m²/d; soybean GPP ranging from 0 to 18 gC/m²/d) [41]. The GPP vs. NDVI $\times$ PAR_{pot}

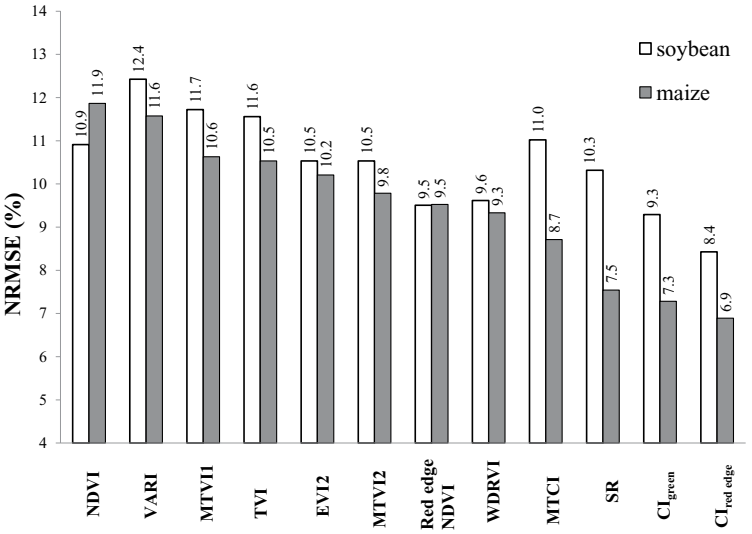

FIGURE 1.14 Normalized root mean square error (NRMSE) of GPP estimation in maize and soybean by vegetation indices. Hyperspectral reflectance data were taken at close range and GPP was measured at three AmeriFlux irrigated and rain-fed sites in Nebraska in 2001 through 2008.

relationship was nonlinear, with slope decreasing as GPP increased. MODIS and Landsat-derived NDVI was a good indicator of low-to-moderate GPP, but it was less accurate in detecting GPP when it exceeded 20 gC/m^2/d. The normalized difference VIs (NDVI, green NDVI, and green WDRVI) performed better than ratio-based VIs (SR and CI_{green}): the NRMSE were >12% for ratio VIs but <8.5% for normalized difference VIs (Table 1.3). Except for green NDVI, all VIs tested in [41] were species specific for maize and soybean. For the same GPP, the value of VI × PAR_{pot} in soybean was consistently higher than that in maize with VIs calculated from reflectance in NIR and red bands. This result is due to contrasting leaf structures and canopy architectures of maize and soybean [11]. Thus, prior information about crop types is required when VIs with red and NIR bands are used for GPP estimation. However, when green band was used in NDVI, the green NDVI vs. GPP

TABLE 1.3

Determination Coefficients (R^2), RMSE, and NRMSE for Relationships GPP vs. VI × PAR_{pot} with VIs Retrieved from TM/ETM+ Landsat Atmospherically Corrected Images Taken over AmeriFlux Maize Sites from 2001 through 2008 and Soybean Sites in 2002, 2004, 2006, and 2008

Vegetation Index	Maize			Soybean		
	R^2	RMSE (gC/m^2/d)	NRMSE (%)	R^2	RMSE (gC/m^2/d)	NRMSE (%)
Green WDRVI	0.95	1.90	6.1	0.90	1.54	8.1
EVI2	0.95	1.92	6.2	0.87	1.79	9.5
Green NDVI	0.94	2.20	7	0.92	1.40	7.5
NDVI	0.93	2.22	7.1	0.89	1.65	8.7
CI_{green}	0.91	2.67	8.5	0.76	2.42	12.3
SR	0.84	3.49	11.0	0.67	2.79	14.2

Note: The vegetation index names are given in full in the text. PAR_{pot}, potential photosynthetically active radiation. RMSE, root mean square error. NRMSE, normalized root mean square error.

relationships for maize and soybean were close, allowing accurate GPP estimation in both crops using the same algorithm (Figure 1.15, Table 1.3).

MODIS 250-m data bring high temporal resolution. To test performance of the model for estimating GPP in irrigated and rain-fed maize and soybean croplands, eight years of MODIS 250-m data were collected and analyzed [40,42]. NDVI, EVI2, WDRVI, and SR were tested in the models. The best performance was found for WDRVI- and EVI2-based models [42] (Figure 1.16).

Thus, our results suggest that about 90% of GPP variation in crops is explained by total canopy Chl content [43–46]. It was also confirmed for wheat [47] and grasslands [48]. Assuming an invariant LUE_{green}, GPP in crops and grasslands may be accurately retrieved from close-range and satellite data [44–45,47–53]. LUE_{green} is affected by many factors, specifically cloudiness coefficient [54] as well as daytime temperature, vapor pressure deficit, and phenology [55]. It was shown that the effect of all these factors on LUE_{green} resulted in normalized standard deviations of LUE_{green} for irrigated and rain-fed maize of 11.9% and for irrigated and rain-fed soybean of 13.3%, thus demonstrating convergence of LUE_{green} to a narrow range [56]. Recently was found that the maximum daily LUE based on PAR absorption by canopy Chl, unlike other expressions of LUE, tends to converge across biome types [57]. Thus, taking into account conservative behavior of LUE_{green}, high accuracy of GPP estimation based on Chl-related vegetation indices and incident or potential PAR it is not surprising.

The question remains: Is a situation of limited resource availability and high resource acquisition costs a reason for efficient resource use and convergence of LUE_{green}? Such a scenario results in an optimization of resource allocation, which then results in a maximization of carbon gains and a convergence on a narrow range of LUE_{green} as was suggested in [58,59]. In this case, the plant response to stress is a decrease in radiation absorbed by photosynthetically active green vegetation such that LUE_{green} remains relatively invariant.

Our results have important implications for remote estimating of primary production in crops. Convergence of LUE_{green} allows the use of simple robust gross primary production models and also a better understanding of the role and constraints of LUE_{green} in process-based models. Assuming invariant LUE_{green}, the models based on either the canopy/stand/community Chl content or green LAI may facilitate accurate assessments of primary production and plant optimization patterns at multiple scales, from leaves to canopies and entire regions.

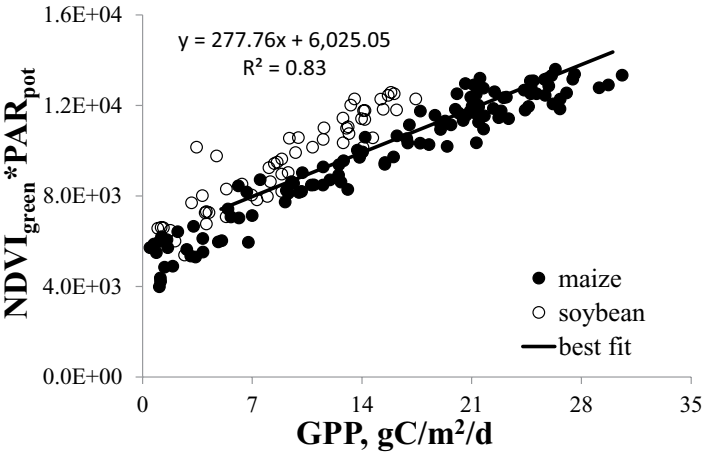

FIGURE 1.15 The relationships between GPP and the product of $NDVI_{green}$ and potential PAR (PAR_{pot}) for maize and soybean. Green NDVI was derived from TM and ETM+ Landsat data taken over irrigated and rain-fed AmeriFlux sites (120 observations over maize and 55 over soybean) from 2001 through 2008.

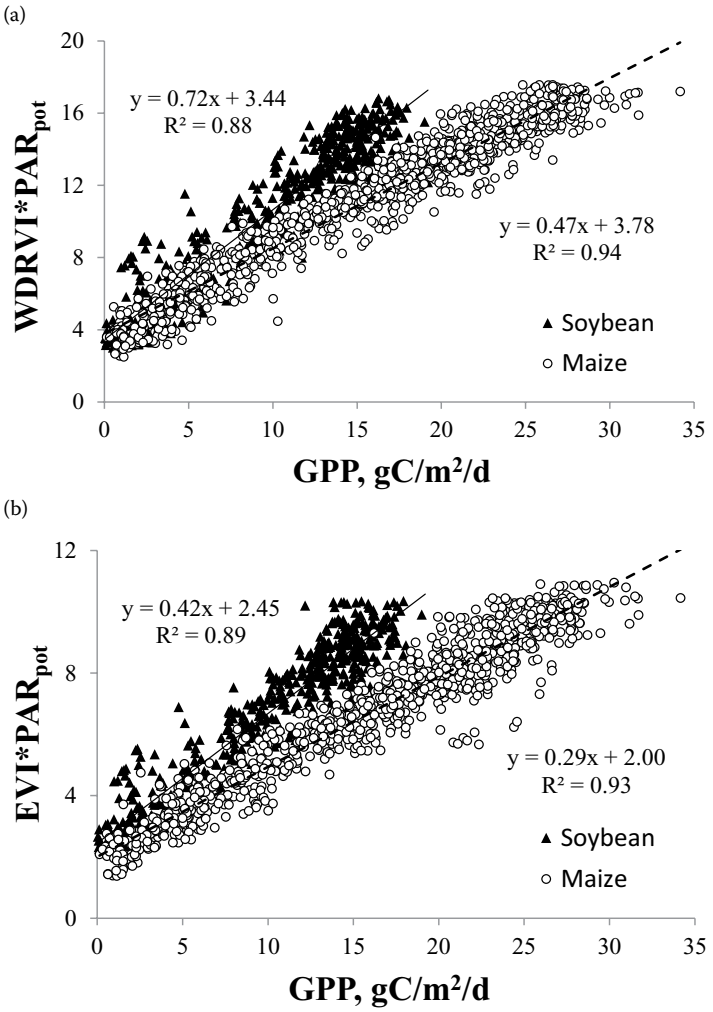

FIGURE 1.16 The product of (a) WDRVI × PAR_{pot}, and (b) EVI × PAR_{pot} plotted versus GPP for 1058 observations over maize and 493 over soybean during growing seasons 2001 through 2008 in Nebraska when (PAR_{po}–PAR_{in})/PAR_{pot} was below 20%. Vegetation indices were retrieved from MODIS 250-m data.

1.7 CONCLUSIONS

Remote sensing techniques for estimating six crop biophysical and biochemical characteristics—vegetation fraction, fraction of PAR absorbed by photosynthetically active vegetation, chlorophyll content, nitrogen content, green leaf area index, and gross primary production—have been presented in this chapter. All techniques were tested using reflectances acquired from close range (6 meters above the top of the canopy) as well as TM/ETM+ Landsat, MODIS, and MERIS satellite data. It was shown that the aforementioned characteristics can be estimated accurately using remotely sensed data. Moreover, generic algorithms were developed that do not require parameterization for crops studied.

Tables 1.1 through 1.3 summarized the accuracy of estimating biophysical characteristics. The choice of index depends on the spectral characteristics of the radiometer or the satellite sensor being used. The indices employing red edge spectral bands, namely, $CI_{red\ edge}$, MTCI, $VARI_{red\ edge}$, $NDVI_{red\ edge}$, and $WDRVI_{red\ edge}$, can be used for satellite systems with spectral bands in the red edge region (Sentinel-2, Sentinel-3, and Venμs). The indices employing green spectral band, namely,

$NDVI_{green}$, $VARI_{green}$, CI_{green}, and $WDRVI_{green}$, can be used for satellite systems with spectral bands in the green region (e.g., Landsat, MODIS 500 m and 1 km spatial resolution, Venμs, Sentinel-2, and Sentinel-3). The indices using only red and NIR spectral bands, namely, NDVI, EVI2, and WDRVI, can be used for crop monitoring by satellite systems such as AVHRR, Landsat, MODIS (250 m spatial resolution) and Venμs.

The implications of these findings are far-reaching since the techniques described open a new possibility for accurate estimation of crop biochemical and biophysical characteristics at different scales, from close range to satellite altitudes. Some of the techniques based on the red, green, and NIR bands allow use of the extensive archive of Landsat and AVHRR imagery acquired since the early 1970s and the 250 m spatial resolution MODIS imagery acquired since 2001.

With these techniques, it is now possible to obtain global synoptic estimates of crop biochemical and biophysical characteristics at 20 and 30 m spatial resolution (Sentinel-2, Landsat TM/ETM+) and at 250 m/300 m resolution (MODIS and Sentinel-3). The performances of the algorithms were tested for maize, soybean, potato, rice, and wheat. These crops have very different canopy architectures and leaf structures. Still, the techniques developed yielded accurate estimations, which indicates that these techniques are likely applicable to other crops as well.

ACKNOWLEDGMENTS

I was honored to work with and learned a lot from Donald C. Rundquist, Shashi Verma, Timothy Arkebauer, and James Schepers. Their help at different stages of this study was invaluable and is greatly appreciated. I acknowledge contributions of my former PhD students Drs. Veronica Ciganda, Anthony Nguy-Robertson, Yi Peng, Andres Vina, and Arthur Zygielbaum. They contributed enormously in development and testing methods and techniques presented here. The support from the Center for Advanced Land Management and Information Technologies and Carbon Sequestration Program at University of Nebraska, USA is appreciated.

REFERENCES

1. Allen, W.A., Gausman, H.W., and Richardson, A.J., Willstatter-Stoll theory of leaf reflectance evaluated by ray tracing, *Applied Optics*, 12, 10, 2448–2453, 1973.
2. Gausman, H.W., Allen, W.A., Myers, V.I., and Cardenas, R., Reflectance and internal structure of cotton leaves Gossypium hirsutum L, *Agron. J.*, 61, 3, 374–376, 1969.
3. Woolley, J.T., Reflectance and transmittance of light by leaves, *Plant Physiology*, 47, 656–662, 1971.
4. Barnes, E.M., Sudduth, K.A., Hummel, J.W., Leach, S.M., Corwin, D.L., Yeng, C.C., Daughtry, S.T., and Bausch, W.C., Remote- and ground-based sensor techniques to map soil properties, *Photogrammetric Engineering and Remote Sensing*, 69, 619–630, 2003.
5. Kustas, W.P., French, A.N., Hatfield, J.L., Jackson, T.J., Moran, M.S., Rango, A., Ritchie, J.C., and Schmugge, T.J., Remote sensing research in hydrometeorology, *Photogrammetric Engineering and Remote Sensing*, 69, 631–646, 2003.
6. Pinter, P.J., Hatfield, J.L., Schepers, J.S., Barnes, E.M., Moran, M.S., Daughtry, C.S., and Upchurch, D.R., Remote sensing for crop management, *Photogrammetric Engineering and Remote Sensing*, 69, 647–664, 2003.
7. Doraiswamy, P.C., Moulin, S., and Cook, P.W., Crop yield assessment from remote sensing, *Photogrammetric Engineering and Remote Sensing*, 69, 665–674, 2003.
8. Moran, S., Fitzgerald, G., Rango, A., Walthall, C., Barnes, E., Bausch, W., Clarke, T. et al., Sensor development and radiometric correction for agricultural applications, *Photogrammetric Engineering and Remote Sensing*, 69, 705–718, 2003.
9. Hatfield, J.L., Prueger, J.H., and Kustas, W.P., Remote sensing of dryland crops. In: S.L. Ustin (ed.), *Remote Sensing for Natural Resource Management and Environmental Monitoring: Manual of Remote Sensing*, 3rd Edition (vol. 4, pp. 531–568). Hoboken, NJ, USA: Wiley, Chapter 10, 2004.
10. Hatfield, J.L., Gitelson, A.A., Schepers, J.S., and Walthall, C.L., Application of spectral remote sensing for agronomic decisions, *Agronomy Journal*, 100, 117–131, 2008, doi: 10.2134/agronj2006.0370c.

11. Gitelson, A.A., Remote sensing estimation of crop biophysical characteristics at various scales. In: P.S. Thenkabail, J.G. Lyon, and A. Huete (eds), *Hyperspectral Remote Sensing of Vegetation* (vol. 1, pp. 329–358). Boca Raton, FL, USA: Taylor & Francis/CRC Press, Chapter 15, 2011.
12. Gitelson, A.A., Remote estimation of crop fractional vegetation cover: The use of noise equivalent as an indicator of performance of vegetation indices, *International Journal of Remote Sensing*, 34, 1–13, 2013, doi: 10.1080/01431161.2013.793868.
13. Gitelson, A.A., Peng, Y., and Huemmrich, K.F., Relationship between fraction of radiation absorbed by photosynthesizing maize and soybean canopies and NDVI from remotely sensed data taken at close range and from MODIS 250 m resolution data, *Remote Sensing of Environment*, 147, 108–120, 2014.
14. Gitelson, A.A., Peng, Y., Vina, A., Arkebauer, T., and Schepers, J.S., Efficiency of chlorophyll in gross primary productivity: A proof of concept and application in crops, *Journal of Plant Physiology*, 201, 101–110, 2016, http://dx.doi.org/10.1016/j.jplph.2016.05.019
15. Liu, X., Guanter, L., Liu, L., Damm, A., Malenovský, Z., Rascher, U., Peng, D., Du, S., and Gastellu-Etchegorry, J.-P., Downscaling of solar-induced chlorophyll fluorescence from canopy level to photosystem level using a random forest model, *Remote Sensing of Environment*, 2018, https://doi.org/10.1016/j.rse.2018.05.035
16. Peng, Y., Nguy-Robertson, A., Arkebauer, T., and Gitelson, A.A., Assessment of canopy chlorophyll content retrieval in maize and soybean: Implications of hysteresis on the development of generic algorithms, *Remote Sensing*, 9, 226, 2017, doi: 10.3390/rs9030226.
17. Inoue, Y., Guerif, M., Baret, F., Skidmore, A., Gitelson, A., Schlerf, M., and Olioso, A., Simple and robust methods for remote sensing of canopy chlorophyll content: A comparative analysis of hyperspectral data for different types of vegetation, *Plant, Cell and Environment*, 39, 2609–2623, 2016, doi: 10.1111/pce.12815.
18. Ciganda, V.S., Gitelson, A.A., and Schepers, J., How deep does a remote sensor sense? Expression of chlorophyll content in a maize canopy, *Remote Sensing of Environment*, 126, 240–247, 2012.
19. Baret, F., Houlès, V., and Guérif, M., Quantification of plant stress using remote sensing observations and crop models: The case of nitrogen management, *Journal of Experimental Botany*, 58, 869–880, 2007.
20. Yoder, B.J., and Pettigrew-Crosby, R.E., Predicting nitrogen and chlorophyll content and concentrations from reflectance spectra (400–2500 nm) at leaf and canopy scales, *Remote Sensing of Environment*, 53, 199–211, 1995.
21. Oppelt, N., and Mauser, W., Hyperspectral monitoring of physiological parameters of wheat during a vegetation period using AVIS data, *International Journal of Remote Sensing*, 25, 145–159, 2004.
22. Clevers, J.G.P.W., and Kooistra, L., Using hyperspectral remote sensing data for retrieving canopy chlorophyll and nitrogen content, *IEEE Journal of Selected Topics in Applied Earth Observations and Remote Sensing*, 5, 574–583, 2012.
23. Clevers, J.G.P.W., and Gitelson, A.A., Remote estimation of crop and grass chlorophyll and nitrogen content using red-edge bands on Sentinel-2 and -3, *International Journal of Applied Earth Observation and Geoinformation*, 23, 344–351, 2013.
24. Schlemmer, M., Gitelson, A.A., Schepers, J., Ferguson, R., Peng, Y., Shanahan, J., and Rundquist, D.C., Remote estimation of nitrogen and chlorophyll contents in maize at leaf and canopy levels, *International Journal of Applied Earth Observation and Geoinformation*, 25, 47–54, 2013.
25. Inoue, Y., Sakaiya, E., Zhu, Y., and Takahashi, W., Diagnostic mapping of canopy nitrogen content in rice based on hyperspectral measurements, *Remote Sensing of Environment*, 126, 210–221, 2012.
26. Viña, A., Gitelson, A.A., Nguy-Robertson, A.L., and Peng, Y., Comparison of different vegetation indices for the remote assessment of green leaf area index of crops, *Remote Sensing of Environment*, 115, 3468–3478, 2011, doi: 10.1016/j.rse.2011.08.010.
27. Nguy-Robertson, A.L., Peng, Y., Gitelson, A.A., Arkebauer, T.J., Pimstein, A., Herrmann, I., Karnieli, A., Rundquist, D.C., and Bonfil, D.J., Estimating green LAI in four crops: Potential of determining optimal spectral bands for a universal algorithm, *Agricultural and Forest Meteorology*, 192–193, 140–148, 2014.
28. Nguy-Robertson, A.L., Gitelson, A.A., Peng, Y., Viña, A., Arkebauer, T.J., and Rundquist, D.C., Green leaf area index estimation in maize and soybean: Combining vegetation indices to achieve maximal sensitivity, *Agronomy Journal*, 104, 1336–347, 2012.
29. Kira, O., Nguy-Robertson, A.L., Arkebauer, T.J., Linker, R., and Gitelson, A.A., Informative spectral bands for remote green LAI estimation in C3 and C4 crops, *Agricultural and Forest Meteorology*, 218–219, 243–249, 2016, http://dx.doi.org/10.1016/j.agrformet.2015.12.064
30. Cai, W., Yankun, Y., and Shao, X., A variable selection method based on uninformative variable elimination for multivariate calibration ofnear-infrared spectra, *Chemometr. Intell. Lab.*, 90, 188–194, 2008.

31. Centner, V., Massart, D.-L., de Noord, O.E., de Jong, S., Vandeginste, B.M., and Sterna, C., Elimination of uninformative variables for multivariate calibration, *Anal. Chem.*, 68, 3851–3858, 1996, http://dx.doi.org/10.1021/ac960321m
32. Kira, O., Nguy-Robertson, A.L., Arkebauer, T.J., Linker, R., and Gitelson, A.A., Toward generic models for green LAI estimation in maize and soybean: Satellite observations, *Remote Sensing*, 9, 318, 2017, doi: 10.3390/rs9040318.
33. Nguy-Robertson, A.L., and Gitelson, A.A., Algorithms for estimating green leaf area index in C3 and C4 crops for MODIS, Landsat TM/ETM+, MERIS, Sentinel MSI/OLCI, and Venμs sensors, *Remote Sensing Letters*, 6, 5, 360–369, 2015, http://dx.doi.org/10.1080/2150704X.2015.1034888
34. Guindin-Garcia, N., Gitelson, A.A., Arkebauer, T.J., Shanahan, J., and Weiss, A., An evaluation of MODIS 8 and 16 day composite products for monitoring maize green leaf area index, *Agricultural and Forest Meteorology*, 161, 15–25, 2012.
35. Verrelst, J., Rivera, J.P., Gitelson, A., Delegido, J., Moreno, J., and Camps-Valls, G., Spectral band selection for vegetation properties retrieval using Gaussian processes regression, *International Journal of Applied Earth Observation and Geoinformation*, 52, 554–567, 2016, http://dx.doi.org/10.1016/j.jag.2016.07.016
36. Gitelson, A.A., Peng, Y., Arkebauer, T.J., and Schepers, J., Relationships between gross primary production, green LAI, and canopy chlorophyll content in maize: Implications for remote sensing of primary production, *Remote Sensing of Environment*, 144, 65–72, 2014.
37. Peng, Y., and Gitelson, A.A., Application of chlorophyll-related vegetation indices for remote estimation of maize productivity, *Agricultural and Forest Meteorology*, 151, 1267–1276, 2011, doi: 10.1016/j.agrformet.2011.05.005.
38. Peng, Y., and Gitelson, A.A., Remote estimation of gross primary productivity in soybean and maize based on total crop chlorophyll content, *Remote Sensing of Environment*, 117, 440–448, 2012, doi: 10.1016/j.rse.2012.10.021.
39. Rossini, M., Migliavacca, M., Galvagno, M., Meroni, M., Cogliati, S., Cremonese, E., Fava, F. et al., Remote estimation of grassland gross primary production during extreme meteorological seasons, *International Journal of Applied Earth Observation and Geoinformation*, 29, 1–10, 2014.
40. Sakamoto, T., Gitelson, A.A., Wardlow, B.D., Verma, S.B., and Suyker, A.E., Estimating daily gross primary production of maize based only on MODIS WDRVI and shortwave radiation data, *Remote Sensing of Environment*, 115, 3091–3101, 2011.
41. Gitelson, A.A., Peng, Y., Masek, J.G., Rundquist, D.C., Verma, S., Suyker, A., Baker, J.M., Hatfield, J.L., and Meyers, T., Remote estimation of crop gross primary production with Landsat data, *Remote Sensing of Environment*, 121, 404–414, 2012.
42. Peng, Y., Gitelson, A.A., and Sakamoto, T., Remote estimation of gross primary productivity in crops using MODIS 250 m data, *Remote Sensing of Environment*, 128, 186–196, 2013.
43. Gitelson, A.A., Peng, Y., Rundquist, D.C., Suyker, A., and Verma, S.B. 2015. Remote estimation of gross primary productivity in maize and soybean: From close range to satellites. In: J.V. Stafford (ed.), *Precision Agriculture'15* (pp. 183–190), Wageningen, Netherlands: Wageningen Academic Publishers, 2015, http://www.wageningenacademic.com/doi/10.3920/978-90-8686-814-8_22
44. Gitelson, A.A., Verma, S.B., Vina, A., Rundquist, D.C., Keydan, G., Leavitt, B., Arkebauer, T.J., Burba, G.G., and Suyker, A.E., Novel technique for remote estimation of CO2 flux in maize, *Geophysical Research Letters*, 30, 9, 1486, 2003, doi: 10.1029/2002GL016543.
45. Gitelson, A.A., Viña, A., Verma, S.B., Rundquist, D.C., Arkebauer, T.J., Keydan, G., Leavitt, B., Ciganda, V., Burba, G.G., and Suyker, A.E., Relationship between gross primary production and chlorophyll content in crops: Implications for the synoptic monitoring of vegetation productivity, *Journal of Geophysical Research*, 111, D08S11, 2006, doi: 10.1029/2005JD006017.
46. Peng, Y., Gitelson, A.A., Keydan, G.P., Rundquist, D.C., and Moses, W.J., Remote estimation of gross primary production in maize and support for a new paradigm based on total crop chlorophyll content, *Remote Sensing of Environment*, 115, 978–989, 2011, doi: 10.1016/j.rse.2010.12.001.
47. Wu, C., Niu, Z., Tang, Q., Huang, W., Rivard, B., and Feng, J., Remote estimation of gross primary production in wheat using chlorophyll-related vegetation indices, *Agricultural and Forest Meteorology*, 149, 1015–1021, 2009.
48. Sakowska, K., Juszczak, R., and Gianelle, D., Remote sensing of grassland biophysical parameters in the context of the sentinel-2 satellite mission, *Journal of Sensors*, 2016, Article ID 4612809, http://dx.doi.org/10.1155/2016/4612809
49. Harris, A., and Dash, J., The potential of the MERIS terrestrial chlorophyll index for carbon flux estimation, *Remote Sensing of Environment*, 114, 1856–1862, 2010.

50. Harris, A., and Dash, J., A new approach for estimating northern peatland gross primary productivity using a satellite-sensor-derived chlorophyll index, *Journal of Geophysical Research*, 116, G04002, 2011, doi: 10.1029/2011JG001662.
51. Rossini, M., Cogliati, S., Meroni, M., Migliavacca, M., Galvagno, M., Busetto, L., Cremonese, E. et al., Remote sensing-based estimation of gross primary production in a subalpine grassland, *Biogeosciences*, 9, 2565–2584, 2012, doi: 10.5194/bg-9-2565-2012.
52. Rossini, M., Migliavacca, M., Galvagno, M., Meroni, M., Cogliati, S., Cremonese, E., Fava, F. et al., Remote estimation of grassland gross primary production during extreme meteorological seasons, *International Journal of Applied Earth Observation and Geoinformation*, 29, 1–10, 2014.
53. Sakowska, K., Vescovo, L., Marcolla, B., Juszczak, R., Olejnik, J., and Gianelle, D., Monitoring of carbon dioxide fluxes in a subalpine grassland ecosystem of the Italian Alps using a multispectral sensor, *Biogeosciences*, 11, 4695–4712, 2014.
54. Suyker, A.E., and Verma, S.B., Gross primary production and ecosystemrespiration of irrigated and rainfed maize–soybean cropping systems over 8 years, *Agricultural and Forest Meteorology*, 165, 12–24, 2012, http://dx.doi.org/10.1016/j.agrformet.2012.05.021
55. Nguy-Robertson, A., Suyker, A., and Xiao, X., Modeling gross primary production of maize and soybean croplands using light quality, temperature, water stress, and phenology, *Agricultural and Forest Meteorology*, 213, 160–172, 2015, http://dx.doi.org/10.1016/j.agrformet.2015.04.008
56. Gitelson, A.A., Arkebauer, T.J., and Suyker, A.E., Convergence of daily light use efficiency in irrigated and rainfed C3 and C4 crops, *Remote Sensing of Environment*, 217, 30–37, 2018, https://doi.org/10.1016/j.rse.2018.08.007
57. Zhang, Y., Xiao, X., Wolf, S., Wu, J., Wu, X., Gioli, B., Wohlfahrt, G. et al., Spatio-temporal convergence of maximum daily light use efficiency based on radiation absorption by canopy chlorophyll, *Geophysical Research Letters*, 45, 3508–3519, 2018, https://doi.org/10.1029/2017GL076354.
58. Field, C.B., Ecological scaling of carbon gain to stress and resources availability. In: H.A. Mooney, W.E. Winner, and E.J. Pell (eds), *Response of Plants to Multiple Stresses* (pp. 35–65). London, UK: Academic Press, 1991.
59. Goetz, S.J., and Prince, S.D., Modelling terrestrial carbon exchange and storage: Evidence and implications of functional convergence in light-use efficiency. In: A.H. Fitter, and D. Raffaelli (eds), *Advances in Ecological Research* (vol. 28, pp. 57–92) San Diego, CA, USA: Academic Press, 1999.